Available online at www.sciencedirect.com

ScienceDirect

Energy Procedia 145 (2018) 345–350

Energy Procedia

www.elsevier.com/locate/procedia

Applied Energy Symposium and Forum, Renewable Energy Integration with Mini/Microgrids, REM 2017, 18–20 October 2017, Tianjin, China

Analysis of MISO Super Lift Negative Output Luo Converter with MPPT for DC Grid Connected Hybrid PV/Wind System

Kumar. K[a], Ramji Tiwari[a], Ramesh Babu. N[b*], Prabhu. K.R[a]

[a]*School of Electrical Engineering, VIT University, Vellore, India;* [b]*M.Kumarasamy College of Engineering,Karur, India.*

Abstract

This paper proposes a multi-input single output (MISO) super lift negative output Luo converter for DC grid connected hybrid wind and photo voltaic (PV) system. The proposed converter is developed by sharing the charging capacitor and DC link capacitor between the two super lift negative output Luo converters to form a hybrid system. Therefore, it has the advantage of the simple structure and reduced converter passive components. The proposed converter is designed and then analyzed for the DC grid connected hybrid wind and PV system. This study considers a 500W wind system and a 560W PV system with maximum power point tracking (MPPT) algorithms of perturb& observe (P&O) method for both wind and PV system. The proposed converter effectiveness has been validated and compared with the proportional integral (PI) and P&O control algorithms by using the simulation results. Based on the availability of the wind and PV energy sources, the converter usage is presented.

Selection and peer-review under responsibility of the scientific committee of the Applied Energy Symposium and Forum, Renewable Energy Integration with Mini/Microgrids, REM 2017

Keywords: super lift Luo converter; wind; Photo Voltaic; MPPT; hybrid system.

1. Introduction

Due to vast energy crises and environmental pollution, renewable energy sources are widely used in domestic, industrial, electric vehicles and other applications where the regular main grid is not available [1,2]. The most promising energy sources among all the renewable energy sources are the wind and solar to meet the load demand, but these sources are uncontrollable and unpredictable in nature, so it is quite difficult to meet the demand individually [3-6].

* N Ramesh Babu. Tel.:+91-9443030636.
E-mail address: nrameshme@gmail.com

Selection and peer-review under responsibility of the scientific committee of the Applied Energy Symposium and Forum, Renewable Energy Integration with Mini/Microgrids, REM 2017
10.1016/j.egypro.2018.04.062

However, this can be defeat by integrating the different renewable energy sources with power electronic converters to form a hybrid system. The most promising renewable energy sources to form a hybrid system are the wind and solar, due to its availability and complement in its nature [7]. The benefit of integration of hybrid renewable energy sources with the grid increase the sustainability, effective peak hour management, electric market up-gradation and reduces the impact on customers during the grid failure. As of June 30^{th,} 2017, the total grid tied installed capacity of wind is 32,508.17MW and the PV is 13,114.82MW. [8]

The voltage generated by these two sources is unstable and too low. So it requires DC-DC converters with high step-up gain to meet the required rating of the system [9,10]. The basic boost converter can increase the voltage gain by operating in its extreme large duty cycle [11,12]. As consequences, stress on the power semiconductor devices increases and decreases the overall conversion efficiency of the system. From the past few decades, several multi-input DC-DC power converter configurations are derived from the traditional buck, boost and buck-boost converters are available and are detailed in the literature [13-17].

In this paper, a new converter topology of MISO super lift negative output Luo converter is proposed for the application of the wind and solar energy sources integration. The advantage of the proposed converter is to operate in both individual and simultaneous modes of operation. The wind energy system is regulated by the switch S_1 with perturb and observer method to extract maximum power and PV energy system is regulated by the switch S_2 with perturb and observer method to extract maximum power.

2. Analysis of super lift negative output Luo converter

The schematic diagram of super lift negative output Luo converter is shown in Fig. 1. It steps up the DC output voltage in geometric progression stage by stage, the converter circuit has one switch, one inductor, two capacitors and two diodes. The transfer gain (G) [18] is given in Eq. (1).

The Luo converter voltage transfer gain,

$$G = \frac{V_o}{V_s} = \frac{1}{1-k} \tag{1}$$

Where, V_s: Source voltage (V), k: Duty cycle, V_O: Output voltage (V), G: Gain value

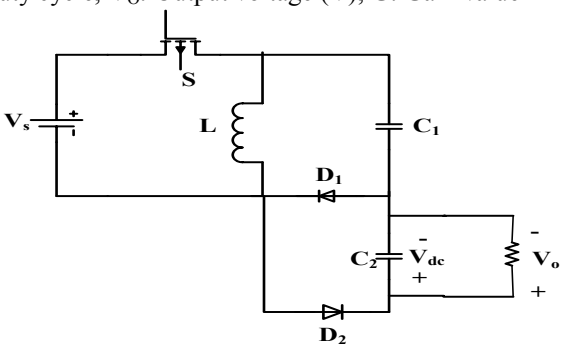

Fig. 1. Super lift negative output Luo converter

2.1 Proposed converter

The schematic diagram of proposed MISO converter is shown in Fig. 2. It is designed from the traditional super lift negative output Luo converter. In order to make a multi-input single output system, two super lift negative output Luo converters are integrated together by sharing the charging capacitor, C_1 and DC link capacitor, C_2 between the two Luo converters as shown in the Fig. 2. It operates in four different modes based on the availability of the energy sources by operating switches S_1 and S_2, as shown in Fig. 3 and are explained in the following sub-section.

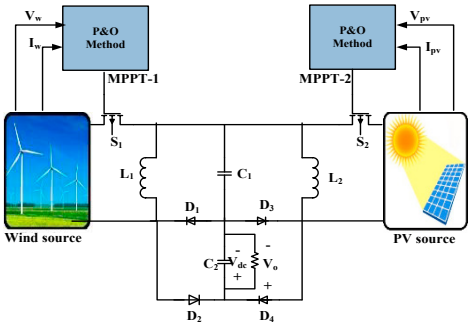

Fig. 2. Block diagram of proposed MISO Luo converter

2.2 Modes of operation

Mode-1: S_1: ON, S_2: ON (Both wind and PV sources are available)

The sharing capacitor C_1 is charged by the both wind and PV source voltages V_w and V_{pv} respectively. i_{L1} is the current flowing through the inductor L_1, increases with the voltage V_w during the availability of wind source and similarly current i_{L2} through inductor L_2, with the voltage V_{pv} during the availability of PV source. The Dc link capacitor, C_2 supplies power to the load. The mathematical current equations ofi_{L1} and i_{L2} are expressed in Eq. (2).

$$i_{L1} = I_w + \frac{V_w + V_{c1}}{L_1} t \quad \text{and} \quad i_{L2} = I_{pv} + \frac{V_{pv} + V_{c1}}{L_2} t \tag{2}$$

Mode-2: S_1: ON, S_2: OFF (wind source alone is available)

When S_1 is ON, the sharing capacitor C_1 is charged by the voltage V_w of the wind source and $i_{L1}$is the current flowing through the inductor L_1 increases with the voltage V_w during the availability of the wind source. When PV source not available, S_2 is OFF, then both C_1 and L_2 are in a discharging state in C_2, to get the boosted voltage across the load. The mathematical current equations of i_{L1} and i_{L2} are given in Eq. (3).

$$i_{L1} = I_w + \frac{V_w + V_{c1}}{L_1} t \quad \text{and} \quad i_{L2} = I_{dc} - \frac{V_{c1}}{L_2} t \tag{3}$$

The summary of modes of operation of proposed converter with switching states is listed in Table 1

Table 1. Summary of modes of operation of the converter

Mode	Wind source	PV source	Diode conduction states				Charging and discharging	
			D_1	D_2	D_3	D_4	L_1	L_2
1	Available (S_1-ON)	Available (S_2-ON)	Forward bias	Reverse bias	Forward bias	Reverse bias	Wind source	PV source
2	Available (S_1-ON)	Unavailable (S_2-OFF)	Forward bias	Reverse bias	Reverse bias	Forward bias	Wind source	Capacitor, C_1
3	Unavailable (S_1-OFF)	Available (S_2-ON)	Reverse bias	Forward bias	Forward bias	Reverse bias	Capacitor, C_1	PV source
4	Unavailable (S_1-OFF)	Unavailable (S_2-OFF)	Reverse bias	Forward bias	Reverse bias	Forward bias	Capacitor, C_1	Capacitor, C_1

Mode-3: S_1: OFF, S_2: ON (PV source alone is available)

When wind source is not available, then S_1 is OFF, then both C_1 and L_1 are in discharging state to C_2, to get the boosted voltage across the load. When PV source is available, S_2 is ON, then the sharing capacitor C_1 is charged by the V_{pv} of the PV source and the current i_{L2} flowing through the inductor L_2, increases with the voltage V_{pv} during

the availability of the PV source. The mathematical current equations of i_{L1} and i_{L2} are given in Eq. (4).

$$i_{L1} = I_{dc} - \frac{V_{c1}}{L_1} t \qquad \text{and} \qquad i_{L2} = I_{pv} + \frac{V_{pv} + V_{c1}}{L_2} t \tag{4}$$

Mode-4: S_1: OFF, S_2: OFF (Both wind and PV sources are not available)

When both sources are not available, then S_1 and S_2 are OFF, then the sharing capacitor and inductor L_1 and L_2 are in discharging state to the DC link capacitor C_2, to get the boosted voltage at the load side. The mathematical current equations of i_{L1} and i_{L2} are given in Eq. (5).

$$i_{L1} = I_{dc} - \frac{V_{c1}}{L_1} t \qquad \text{and} \qquad i_{L2} = I_{dc} - \frac{V_{c1}}{L_2} t \tag{5}$$

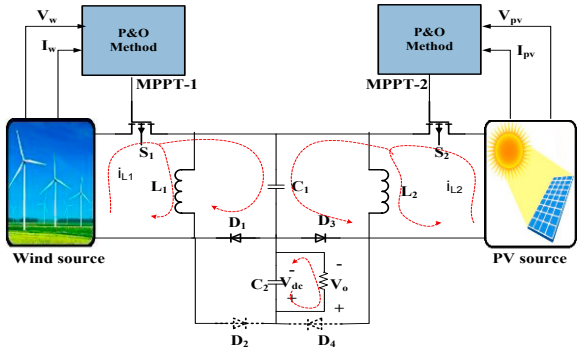

(a)Mode-1: S_1: ON, S_2: ON (Both wind and PV sources are available)

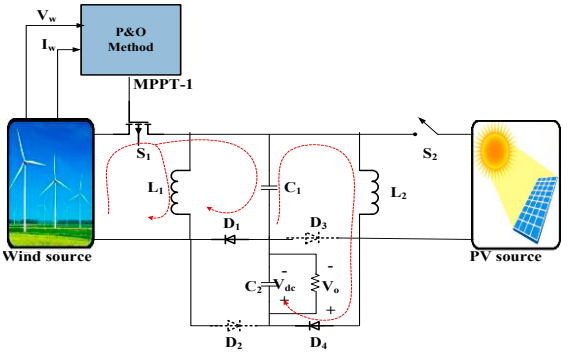

(b) Mode-2: S_1: ON, S_2: OFF (wind source alone is available)

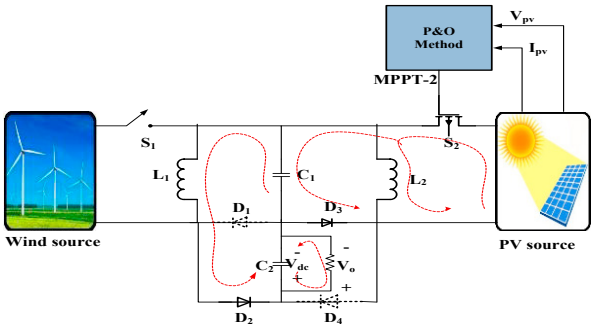

(c) Mode-3: S_1: OFF, S_2: ON (PV source alone is available)

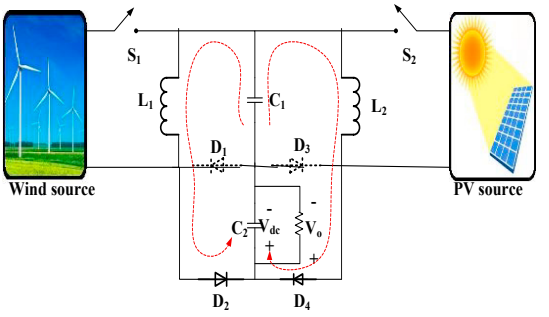

(d)Mode-4: S_1: OFF, S_2: OFF (Both sources are not available)

Fig. 3. (a)-(d) Modes of operation of proposed MISO Luo converter

3. Simulation result analysis

The performance of the proposed MISO Luo converter is validated by considering the availability of wind speed as constant 12m/sec for the period of 0 to 0.4 sec and the solar irradiation is 1000 w/m^2 for the period of 0.4 to 0.8 sec. The proposed hybrid system parameter specifications are listed in Table 2.

Table 2. Hybrid system parameter specifications

Description	Ratings
PV rating	24 V, 23.4 A, 560 W
Wind rating	24 V, 21 A, 500 W
Luo converter-1	L_1=3e^{-3} H
Luo converter-2	L_2=3e^{-3} H
Sharing capacitor	C_1=1e^{-3} F
DC link capacitor	C_2=5e^{-3} F
Load resistance	R=110 Ω
Switching frequency	f_s=15 kHz

In region (0 to 0.4 sec), the wind is the only source available energy source, it varies continuously as per the availability of energy source. In this region wind system with Luo converter-1 is in operating state and step up the available 24V wind source to 240V DC by operating at its voltage transfer gain of 10 as shown in Fig.4.

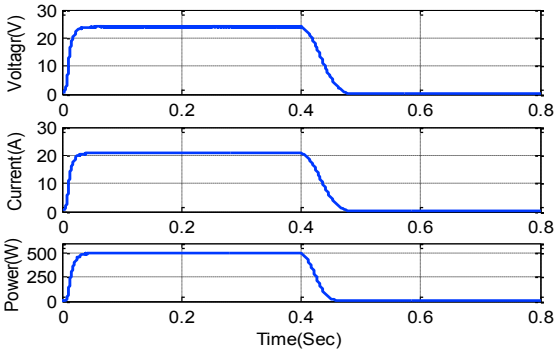

Fig. 4. Wind system output voltage, current and power

In region (0.4 to 0.8 sec), PV is the only available energy source; it varies continuously as per the availability of energy source. In this region, PV source with Luo converter-2 is in operating state and step up the available 24 V PV source to 240 V DC by operating at its voltage transfer gain of 10 as shown in Fig. 5.

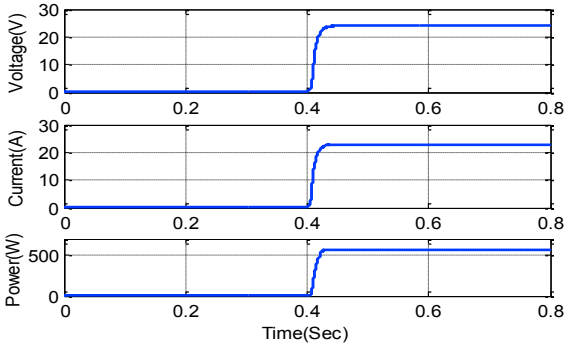

Fig. 5. PV system output voltage, current and power

Fig. 6 shows that the output voltage of the hybrid system is kept constant despite the variation in the input sources. During the period 0 to 0.4 sec, wind source will provide input to the converter and PV source provides for the period 0.4 to 0.8 sec. the MPPT control algorithm used in this paper are P&O and PI. The comparison of the both the control algorithms for the proposed converter are shown in Fig. 6.

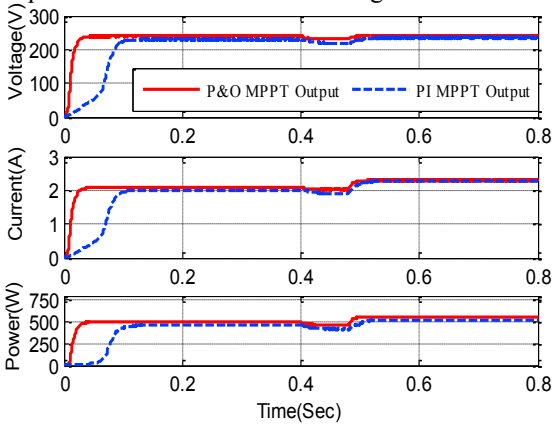

Fig. 6. DC link voltage, current and power

Table 3, compute the results obtained by the proposed converter while using P&O and PI control algorithms. From the table, it is seen that the P&O based MPPT algorithm with proposed converter gives the average maximum power of 516W, while the PI controller gives the only 468W. Thus the proposed converter along with the P&O based MPPT algorithm provides the better performance.

Table 3. Comparison of MISO hybrid system with MPPT

	Wind system output	PV system output	Average output with MPPT	
			PI	P&O
Voltage (V)	240	240	235	240
Current (A)	2.1	2.34	1.98	2.15
Power (W)	500	560	468	516

4. Conclusion

The analysis of MISO Luo converter with MPPT has been presented for DC grid connected wind and PV hybrid system. In this paper, two super lift negative output Luo converters are integrated together to minimize the converter components and for the application of renewable energy sources integration. Based on the availability of energy sources, control switches S_1 and S_2 decides the mode of operation of the proposed converter. MPPT P&O method has been realized for the both PV and wind system and the results are compared with the PI-based MPPT technique. The proposed converter with the P&O algorithm as an MPPT shows the better performance by making the use of complementary nature of renewable energy sources and maintains constant 240 DC throughout the period.

References:

[1] Haitham AR., Malinowski M., and Kamal AL.,. Power electronics for renewable energy systems, transportation and industrial applications. *John Wiley & Sons*. 2014.
[2] Saravanan, S., Babu NR. Analysis and implementation of high step-up DC-DC converter for PV based grid application. *Appl Energy. 2017;* 190: 64-72.
[3] Tiwari R, and Babu NR. Fuzzy Logic Based MPPT for Permanent Magnet Synchronous Generator in wind Energy Conversion System. *IFAC-Papers OnLine*. 2016; 49(1): 462-467.
[4] Erdinc O., Uzunoglu M. Optimum design of hybrid renewable energy systems: Overview of different approaches. *Renew. Sustain. Energy Rev*. 2012; 16(3): 1412-1425.
[5] Tiwari R, Babu NR. Recent developments of control strategies for wind energy conversion system. *Renew. Sustain. Energy Rev*. 2016; 66 : 268-285.
[6] Kumar K., Babu NR, Prabhu KR. Design and Analysis of an Integrated Cuk-SEPIC Converter with MPPT for Standalone Wind/PV Hybrid System. *Int. J Renew Energy Research*. 2017; 7(1): 96-106.
[7] Kumar K., Babu NR., Prabhu KR. Design and Analysis of RBFN Based Single MPPT Controller for Hybrid Solar and Wind Energy System. *IEEE Access.*2017; 5: 15308 - 15317.
[8] Cumulative development of various renewable energy system/ devices in country. Retrieved from *http://mnre.gov.in/mission-and-vision-2/achievements*. 30 June 2017.
[9] Wu .G, Xinbo Ruan, and Zhihong Ye. Nonisolated high step-up dc–dc converters adopting switched-capacitor cell. *IEEE trans indus electron*. 2015; 62(1): 383-393.
[10] Liang, Tsorng-Juu, Jian-Hsieng Lee, Shih-Ming Chen, Jiann-Fuh Chen, and Lung-Sheng Yang. Novel isolated high-step-up DC–DC converter with voltage lift. *IEEE trans indus electron*. 2013; 60(4): 1483-1491.
[11] Saravanan, S., Babu NR. RBFN based MPPT algorithm for PV system with high step up converter. *Energy Convers Manag*. 2016; 122: 239-251.
[12] Saravanan, S., Babu NR. Non-Isolated DC-DC Converter for Renewable Based Grid Application. *Energy Procedia*. 2016; 103: 310-315.
[13] Zhang, Neng, Danny Sutanto, and Kashem M. Muttaqi. A review of topologies of three-port DC–DC converters for the integration of renewable energy and energy storage system. *Renew. Sustain. Energy Rev*. 2016; 56: 388-401.
[14] Akar, Furkan, et al. A Bidirectional Nonisolated Multi-Input DC–DC Converter for Hybrid Energy Storage Systems in Electric Vehicles. *IEEE Trans Vehicular Technol*. 2016; 65(10): 7944-7955.
[15] Liu, Fuxin, Zhicheng Wang, Yunyu Mao, and Xinbo Ruan. Asymmetrical half-bridge double-input DC/DC converters adopting pulsating voltage source cells for low power applications. *IEEE Trans Power Electron*. 2014; 29(9): 4741-4751.
[16] Chen, Yen-Mo, Alex Q. Huang, and Xunwei Yu. A high step-up three-port dc–dc converter for stand-alone PV/battery power systems. *IEEE Trans Power Electron*. 2013; 28(11): 5049-5062.
[17] Khosrogorji, S., M. Ahmadian, H. Torkaman, and S. Soori. Multi-input DC/DC converters in connection with distributed generation units–A review. *Renew. Sustain. Energy Rev*.. 2016; 66: 360-379.
[18] Rashid, Muhammad H. Power electronics handbook: devices, circuits and applications. *Academic press*, 2010.